



HAL
open science

Modelling forest fire and firebreak scenarios in a mediterranean mountainous catchment: Impacts on sediment loads

Thomas Grangeon, Rosalie Vandromme, Olivier Cerdan, Anna Maria De Girolamo, Antonio Lo Porto

► To cite this version:

Thomas Grangeon, Rosalie Vandromme, Olivier Cerdan, Anna Maria De Girolamo, Antonio Lo Porto. Modelling forest fire and firebreak scenarios in a mediterranean mountainous catchment: Impacts on sediment loads. *Journal of Environmental Management*, 2021, 289, 10.1016/j.jenvman.2021.112497. hal-03746475

HAL Id: hal-03746475

<https://brgm.hal.science/hal-03746475>

Submitted on 5 Aug 2022

HAL is a multi-disciplinary open access archive for the deposit and dissemination of scientific research documents, whether they are published or not. The documents may come from teaching and research institutions in France or abroad, or from public or private research centers.

L'archive ouverte pluridisciplinaire **HAL**, est destinée au dépôt et à la diffusion de documents scientifiques de niveau recherche, publiés ou non, émanant des établissements d'enseignement et de recherche français ou étrangers, des laboratoires publics ou privés.



Research article

Modelling forest fire and firebreak scenarios in a mediterranean mountainous catchment: Impacts on sediment loads

Grangeon Thomas^{a,*}, Vandromme Rosalie^a, Cerdan Olivier^a, De Girolamo Anna Maria^b,
Lo Porto Antonio^b

^a Bureau de Recherches Géologiques et Minières, Département Risques et Prévention, 3 Avenue Claude Guillemin, 45100, Orléans, France

^b Water Research Institute, National Research Council, Francesco De Blasio 5, 70132, Bari, Italy



ARTICLE INFO

Keywords:

Soil erosion
Runoff
Forest fires
Firebreaks
Flood events

ABSTRACT

Forests provide a number of ecological and hydrological services, for instance, contributing to decreased water and sediment yields through increased infiltration and reduced soil erosion. However, forest fires can turn positive forest services into drawbacks, enhancing surface runoff and soil erosion and damaging both hillslopes and downstream aquatic life in rivers. Therefore, appropriate mitigation strategies should be developed to limit these negative effects. Using a runoff and erosion model (the WaterSed model), we proposed forest fire and firebreak scenarios to analyse their respective effects on sediment loads. The model reproduced the measured discharge and sediment loads over an entire hydrological year, including 21 flood events occurring from November 2010 to May 2011 in a 72-km² Mediterranean catchment (Celone catchment, Puglia, Italy). Eight different forest fire scenarios were then proposed. While the mean burnt areas remained below 2% of the total catchment area, forest fires significantly affected the sediment yield. Indeed, the sediment yield increased over the different forest fire scenarios, from 1.97 to 2.70 t ha⁻¹.yr⁻¹, corresponding to a 37% increase. At the flood-event scale, the sediment load after fire represented up to 324% of the unburnt catchment sediment load in the worst-case scenario. By using realistic firebreaks, the sediment load could be dramatically reduced, from 324% to 165%, in the worst-case scenario. Because rural catchments, such as the Celone catchment, are currently experiencing land abandonment, forested areas are expected to replace crops and expand in the future. This change will likely increase forest ecological services, which may, however, be punctually balanced by negative fire effects. More studies addressing the global impacts of forest growth, fires and firebreaks on sediment transfers are therefore needed in similar environments.

1. Introduction

Forests provide a number of ecological services, including enhanced infiltration and water retention, therefore contributing to water quality through filtration within the soil column (Bredemeier et al., 2011) and making forests effective agents of flood hazard reduction (Farley et al., 2005; Schüler et al., 2006). The combined effects of vegetation, litter cover and reduced water yield imply decreased erosion rates under forest cover, affecting both the soil quality and the downstream aquatic environments (Owens et al., 2005).

However, Mediterranean countries are recurrently facing forest fire issues. For instance, approximately 4400 km² were, on average, burnt each year across France, Portugal, Spain, Italy and Greece during the period of 1985–2016 (EEA, 2019). Italy represented, on average,

approximately 960 km² (ISPRA, 2020). Fires can seriously affect ecosystems (Pausas and Keeley, 2009) and the ability of forests to reduce soil erosion. It can be problematic given that forest fire occurrence may increase under future climate change (Flannigan et al., 2009), particularly in Mediterranean countries (Turco et al., 2014). In Italy, it has been noted that the highest number of forest fires and the largest burnt surface area occur in the years with the lowest rainfall and highest maximum temperature (ISTAT, 2010). Forest fires have been demonstrated to affect soil properties (Certini, 2005), enhancing hydrophobicity, resulting in decreased infiltration capacity, increased runoff (Martin et al., 2001) and increased hydrological connectivity (Fernández et al., 2020). Moreover, vegetation and litter burning combined with organic matter removal from soils result in higher soil erodibility. Consequently, forest fires highly increase erosion rates (Pausas et al.,

* Corresponding author.

E-mail address: t.grangeon@brgm.fr (G. Thomas).

<https://doi.org/10.1016/j.jenvman.2021.112497>

Received 11 December 2020; Received in revised form 5 March 2021; Accepted 26 March 2021

Available online 3 April 2021

0301-4797/© 2021 The Authors.

Published by Elsevier Ltd.

This is an open access article under the CC BY-NC-ND license

(<http://creativecommons.org/licenses/by-nc-nd/4.0/>).

2008; Shakesby et al., 2011; Vieira et al., 2015).

To improve our understanding of forest fire effects on runoff and erosion and provide tools to design relevant mitigation strategies against this threat, numerical model developments are needed. Several models have thus been developed or adapted to address this research topic, especially at the plot and hillslope scales (e.g., Larsen and MacDonald, 2007; Robichaud et al., 2007; Fernandez et al., 2010; Esteves et al., 2012; Vieira et al., 2014; Fernández and Vega, 2016; Vieira et al., 2018), for which data are available or easy to collect. However, very little data, including those for pre- and post-fire situations, are available at the catchment scale (Nunes et al., 2020), hampering the possibility of analysing the net impact of forest fires on runoff, soil erosion, and sediment dynamics as well as the possibility of testing numerical models at this scale.

Consequently, little modelling research has addressed forest fire effects on sediment dynamics at the catchment scale. Van Eck et al. (2016) used LISEM to model the post-fire response of a micro-catchment (11 ha) scale but did not simulate sediment dynamics. Salis et al. (2019) applied ERMiT to numerous hillslopes over a 680-km² area but did not simulate the hillslope-river continuum. Nunes et al. (2018) demonstrated the impact of forest fires in the context of afforestation in a relatively small catchment (94 ha) using the SWAT model. More recently, Basso et al. (2019) used the SWAT model to address this issue at two large scales (approximately 210 km² and 3000 km²). However, these scales prevented a detailed analysis of the within-catchment land-use heterogeneities, which might have impacted sediment connectivity (Baartman et al., 2020) and therefore sediment yield.

Land-use heterogeneities may have natural or anthropic origins (e.g., crops in lowlands and forests on steep mountainous slopes), arising from forest fires (burnt and unburnt forest patches) and from the use of firebreaks designed to prevent forest fire expansion. Firebreak examples include soil ploughing, large tree cutting within forests, trafficable paths or roads and mineral earth (Smith, 2014). The use of firebreaks also includes prescribed burning (Matsypura et al., 2018) and strips of low-flammability vegetation. The latter can provide environmental benefits in addition to reducing fire propagation (Curran et al., 2018; Cui et al., 2019).

As forest fires may not always be fully contained and given the potential deleterious effects of sediments and ashes transferred to river systems following fires (Verkaik et al., 2013), it is important to demonstrate that models can be used to quantify the effects of firebreaks on sediment yield at the catchment scale. Moreover, Kampf et al. (2020) compared four different models and showed that these models were able to quantify low and high erosion potential within catchments, such as burnt areas, meaning that models might be useful tools that can be used to describe the spatial patterns of erosion at the catchment scale and, therefore, to analyse sediment connectivity. Consequently, the models might now be used as tools to design and analyse strategies to reduce deleterious forest fire effects, an approach that has not been previously used.

The objectives of this study were twofold. First, we analysed the effects of forest fires on sediment fluxes at the catchment scale based on multiple measured rainfall events over the course of a hydrological year. Second, we analysed the effects of firebreaks on sediment loads. The results provide new insights into soil erosion impacts on sediment connectivity at the catchment scale.

2. Material and methods

2.1. Rationale for the numerical study methodology

The current study aimed to study the effects of forest fires on soil erosion and sediment yield at the catchment scale. The objective was to design plausible forest fire and firebreak scenarios. We therefore chose to use measured data (rainfall, discharge, suspended sediment concentration) and designed forest fire scenarios using the existing catchment

characteristics (land use, soils, topography, roads and village locations) instead of designing hypothetical scenarios. This choice was made i) to design realistic modelling scenarios and recommendations and ii) because, in the studied catchment, as in many comparable Mediterranean rural environments, forests are located in difficult-to-access areas with steep slopes and are therefore unlikely to be trafficable. We therefore chose not to analyse scenarios in which firebreaks would be placed, for instance, every 100 m or by dividing forest patches in equal areas, as can be achieved in the plains.

2.2. The Celone catchment: overview and previous results

The Celone catchment is located in the Puglia region in southern Italy. The basin was recognised as an area of high risk for wildfire in the regional analysis developed by the Civil Protection Agency Regional Plan 2018–2020. The zone designation is based on factors that affect the probability that the area could be burned and the potential fire behaviour that is expected. Several factors are considered, such as fire history, type of vegetation (e.g., conifers and deciduous forests), existing and potential fuels, terrain, and weather conditions. The causes of the fires are attributable to the intentional and negligent or imprudent behaviour of farmers, tourists, and local citizens. The Regional Authority promulgated a Law and published guidelines to prevent wildfires (Regione Puglia, Legge N. 38 December 12, 2016). Among the regulations, the Law imposes a general ban on the burning of arable stubble or other agricultural wastes within the whole Region from 1st June to the end of September with a few derogations. In the latter cases, specific guidelines define the necessary security measures. In some cases, farmers do not adopt all security measures, thus putting the nearby forests at risk. However, in this study, we considered that fires could affect only forests and not agricultural lands. Indeed, because of their location and limited accessibility, burnt forests are likely not to be managed; rather, they are left for vegetation regrowth. Conversely, agricultural lands, mostly located in plains, could be easily managed, for instance, through ash removal and ploughing. The effects of fires on agricultural areas are therefore expected to be limited in time and are thus not considered in our study, in which we address the impacts of fires over the course of a hydrological year. In the study area, due to environmental factors, fires can spread rapidly, making them very difficult to control. Consequently, in this study, we considered that the fire intensity was high for the forest fire scenarios.

For a detailed catchment description, the reader is referred to De Girolamo et al. (2015). In brief, the studied catchment area is 72 km² at the monitoring station. The lithology is mainly composed of flyschoid formations, green-blue clays and alluvial deposits. The soil texture is sandy-clay-loam, clay-loam or clay, and the main soil types are Typic Haploxeroll, Vertic Haploxerept and Typic Calcixeroll.

The elevation ranges from 185 m to 1135 m. The higher slopes (up to 63%) are concentrated in the upper part of the catchment while the lower part is mainly a hilly alluvial plain (median slope is 8%). The catchment is covered with agricultural fields (55%), pastures (6%) and forests (37%, including olive, deciduous and coniferous trees), mainly located in the upper part of the catchment (Fig. 1).

The Celone River originates from the upper, mountainous part of the catchment and flows downstream into a steep valley and then to the agricultural part of the catchment, where the width increases. The total river length of the main stream upstream of the dam is 27 km. The main road is from the lower part of the catchment to Faeto, and its total length is 30 km. The secondary road connects the main road to Celle San Vito. It also has an eastern part. Its total length is 12 km. Only part of the river and part of the main road are located next to forests, while the secondary road is surrounded by forest.

The mean annual precipitation for the 1960–2000 period was 795 mm in the upper part of the catchment and 653 mm in the lower part of the catchment. Rainfall mainly (70%) occurred between November and May. The mean annual temperatures ranged from 3.4 °C to 25.5 °C.

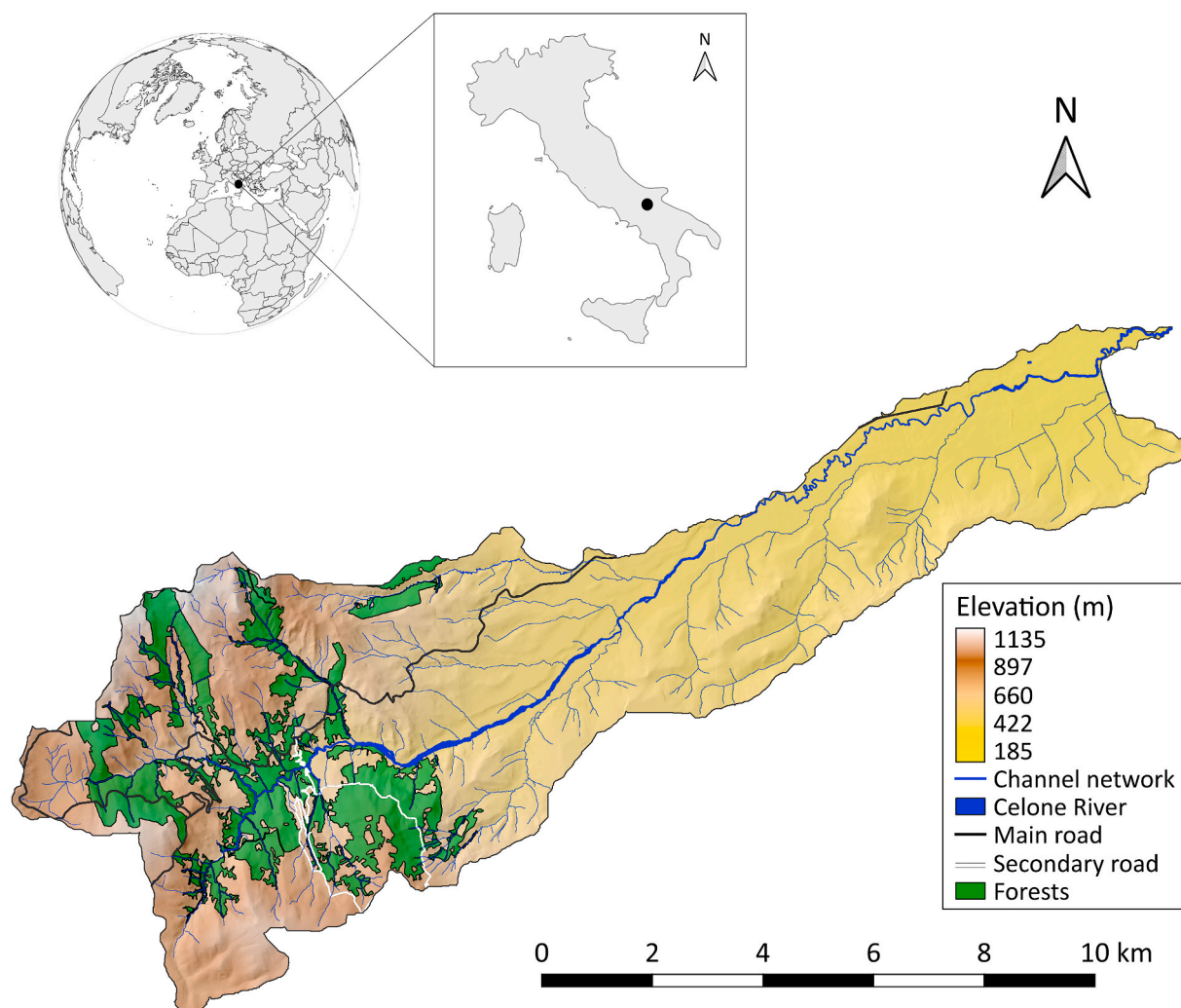


Fig. 1. Overview of the Celone catchment: location, elevation (colour scale), forests (green areas), main channel networks and the Celone River (blue lines and area, respectively), main and secondary roads (black and white lines, respectively). (For interpretation of the references to colour in this figure legend, the reader is referred to the Web version of this article.)

This catchment was previously studied both experimentally and numerically. Among these studies, [De Girolamo et al. \(2015\)](#) demonstrated the high erosivity and sediment dynamics of this catchment, characterised by a fast hydrological response. In summer, flash floods that occur in a few hours are common, during which water transports a large amount of sediment. The sediment yield ranged from 2.40 to 6.06 $t\ ha^{-1}\ yr^{-1}$ ([De Girolamo et al., 2018](#)). It was also shown that these fluxes occurred mainly during the high flow regime, and the low flow regime represented less than 0.1% of the fluxes. The sediment fluxes were mainly recorded between November and May. Another study including this catchment ([De Girolamo et al., 2017](#)) analysed the potential impact of future climate change (2030–2059) on the water balance components under a predicted 0.5–2.4 °C temperature increase and 4–7% precipitation decrease. This result showed that climate change is likely to result in decreased high-flow magnitudes and an increase in dry seasons associated with reduced snowfall and increased evapotranspiration (4%). Consequently, fire risk is expected to be maintained, or even increase, in this region in the future because drier periods are usually associated with larger burned areas per year ([Pausas et al., 2004](#)).

2.3. Monitoring station and data analysis

A hydrological station was installed in the lower part of the

catchment from July 2010 to July 2011, and discharge was recorded at a 5-min time step (ISCO 750 Area Velocity Flow Module). Water samples were collected in the river section using an automatic sampler during and between flood events (ISCO sampler 6712FS), and the suspended sediment concentration was determined in the laboratory. Twenty-one flood events with coupled rainfall – discharge – suspended sediment concentration measurements were recorded. Rainfall was recorded at a 30-min time step by two rainfall gauges. It was spatialized at the sub-basin level as developed in the SWAT model application, which assigned a rainfall gauging station for each sub-basin using the centroid method. The measured flood events were identified from continuous measurements using the methodology described in [Grangeon et al. \(2017\)](#). It is based on the relative proportion of baseflow, calculated using the methodology described in [Chapman \(1991\)](#), using a recursive digital filter. In short, a flood event was identified based on a threshold on the quick-flow/baseflow proportion and was associated with rainfall events, identified based on a threshold on rainfall depth and duration. Baseflow was removed from flood events before processing. For each storm event, the following characteristics were calculated: rainfall depth (mm), rainfall duration (minutes), maximum rainfall intensity ($mm\ h^{-1}$), flow volume (m^3 or mm), flow duration (h), peak discharge ($m^3\ s^{-1}$), runoff coefficient (%), and sediment load ($t\ ha^{-1}$). Sediment yield ($t\ ha^{-1}\ yr^{-1}$) was calculated using the sum of the 21 flood events. It can be considered an acceptable hypothesis given that it was demonstrated

that most of the sediment fluxes generally occurred during flood events in headwater catchments (Navratil et al., 2011; Grangeon et al., 2017), particularly in the Celone catchment, where 94% of suspended material was transported during the high flow regime (De Girolamo et al., 2015). These characteristics are provided as Supplementary material.

A statistical analysis based on a Pearson and Spearman correlation matrix (provided as Supplementary material) was performed to analyse the main factor affecting runoff and sediment load. The result suggested that both infiltration excess and saturation excess occurred during the monitoring period and that sediment loads were strongly controlled ($R^2 = 0.86$) by the water yield. Consequently, although this study focused on erosion and sediment transport, the model was first calibrated on water yield and then on sediment load.

The normality of regression residuals was tested using the Shapiro-Wilk test, and regression quality was evaluated using the coefficient of determination.

2.4. Land use and forest fires scenarios

This study was performed in two steps. First, scenario 1 corresponded to the baseline scenario, in which the model was calibrated against measured data over the 2010–2011 period using the observed land use. The corresponding rainfall event characteristics and model parameters were unchanged in the following scenarios. Some of the model inputs were, however, changed to consider forest fires (Section 2.5). In a second step, different forest fire scenarios were performed to analyse the effect of fires on sediment fluxes. In these scenarios, homogeneous forest patches were defined (Fig. 2).

In the following, it was assumed that the burnt forest characteristics did not change over the different flood events. This hypothesis is based on the relatively low time period of the current study, performed over a unique hydrological year, under high severity forest fire (Section 2.2). Indeed, although vegetation will regrow after fire, Mayor et al. (2007) and Pausas et al. (2008) showed that erosion might be two orders of magnitude higher even five years after fire. This result was associated with a total plant cover lower than 40% after one year, indicating that the vegetation regrowth impact on erosion over a year should be limited for a high severity forest fire.

Forest patches were considered connected, relative to fire propagation, as long as they were within or less than a 15-m radius of another forest patch, based on recommended values for firebreaks (Wilson 1988; Scott et al., 2012; Cawson et al., 2013; Morvan, 2015), and particularly for forest firebreaks (Smith, 2014).

In scenario 2, no firebreaks were considered. In scenarios 4, 6 and 8, it was considered that the main Celone River channel was sufficiently large to act as a natural firebreak. In scenarios 3 to 8, various road combinations were considered as artificial firebreaks. Indeed, in this catchment, the roads are well maintained, with little vegetation left on the road borders, and the roads can be easily used by firefighters. Moreover, the trafficable width is larger than 5 m on the two main roads, which connect the main villages with the valley (Faeto for the main road and Celle San Vito for the secondary road). They can therefore be considered firebreaks and useable by firefighters under forest fire scenarios (Smith, 2014). This value is smaller than the 15-m radius previously defined because vegetation can exist between forest patches (e.g., grasslands), favouring fire propagation, which will likely not be the case over roads. Various combinations of these firebreaks were made to cover a wide range of possible scenarios (Table 1).

Because forest fires could occur anywhere in the catchment, in the fire scenarios, each patch was considered to be affected by fires. Consequently, for each scenario described in Table 1, one model run was performed including one burnt patch, successively for each flood event and each patch. For instance, 7 runs were performed considering 7 different burnt patches in scenario 2 for each flood event; 19 runs were performed for each flood event, corresponding to 19 patches in scenario 8. This approach resulted in 93 simulations for each of the 21 monitored

flood events: the baseline scenario and 92 forest fire model runs, corresponding to the sum of the burnt patches. All of the scenario maps and the burnt patches are included in the Supplementary material.

The sediment connectivity index (Borselli et al., 2008; Cavalli et al., 2013) was calculated using the SedInConnect tool (Crema and Cavalli, 2018) because forest fires have been demonstrated to increase sediment connectivity (Ortiz-Rodríguez et al., 2019). This index describes the potential downward transport of the sediment that is produced upslope, taking into account the contributing area, slope gradient and flow path length. The USLE C-factor (Wischmeier and Smith, 1978) was used as a weighting factor (Baartman et al., 2020), using a mean value of 0.3 for crops (Gabriels et al., 2003), 0.003 for forests (Borelli et al., 2016), and 0.3 for burnt forests (Larsen and MacDonald, 2007). The 99th percentile of the connectivity maps was calculated for each model run, representing a synthetic value of connectivity over the catchment (De Walque et al., 2017), hereafter referred to as the connectivity index. To evaluate the fire effects on connectivity, the connectivity index was restricted to the forested part of the catchment.

2.5. Model set-up

The Watersed model (Baartman et al., 2020; Landemaine et al. in prep.) is an event-based model simulating runoff and soil erosion at the catchment scale. It is raster-based and describes runoff, erosion and sediment transport based on hydrological and sediment balances. Infiltration-excess and saturation-excess runoff are considered, including runoff infiltration and sheet and gully erosion. In this study, the raster resolution was 8 m, based on the resolution of the initial digital elevation model (DEM), which was downloaded from a national database (www.sit.puglia.it).

Based on the measured data analysis, the rainfall depth and duration were used as inputs for the storm events. As the model was designed to reproduce runoff dynamics, the results were compared to the measured quick flow, i.e., after baseflow removal. The DEM was pre-processed following field observations of the runoff network to include small-scale features likely to affect the runoff pathways (e.g., flow of ditches through culverts across roads).

Land-use and pedological maps were downloaded from the same database as the DEM. The land-use map was completed with the topographic map for roads, tracks, and urban areas. Cutting-based farmer interviews and field surveys were also carried out to distinguish arable land types (durum wheat, sunflowers and tomatoes). Soil maps were reclassified according to hydrological soil groups (USDA, 1985; map provided in Supplementary material), soil texture and land use to define land use units. These units were used to define soil properties. The soil water storage capacity was estimated based on the model using the slopes proposed by Saulnier et al. (1997).

Infiltration-excess runoff was considered using the infiltration capacity attributed to the different land use units. Although the model is event-based, saturation-excess runoff was considered by successive simulations of the 21 flood events. The model was run for the 21 measured flood events, and the infiltrated water volume filled the water storage during each simulation. Between events, the water storage was emptied using evapotranspiration, calculated using the simple Thornthwaite (1948) equation. Indeed, this equation requires limited (i.e., temperature) and generally available inputs, and it has been shown to provide interesting results relative to 27 other formulations of various complexities (Oudin et al., 2005). In this equation, the heat index was based on the mean temperature over the full period of 1987–2014, while the average daily temperature was based on the 2010–2011 values, corresponding to the monitoring period.

At the basin scale for the current condition (pre-fire), Watersed was calibrated by using measured data (discharge and suspended sediment concentration). For forest fires, the model was implemented by changing the infiltration capacity, Manning's n and soil erodibility, as reported in the literature. The final inputs resulted in the burnt values for infiltration

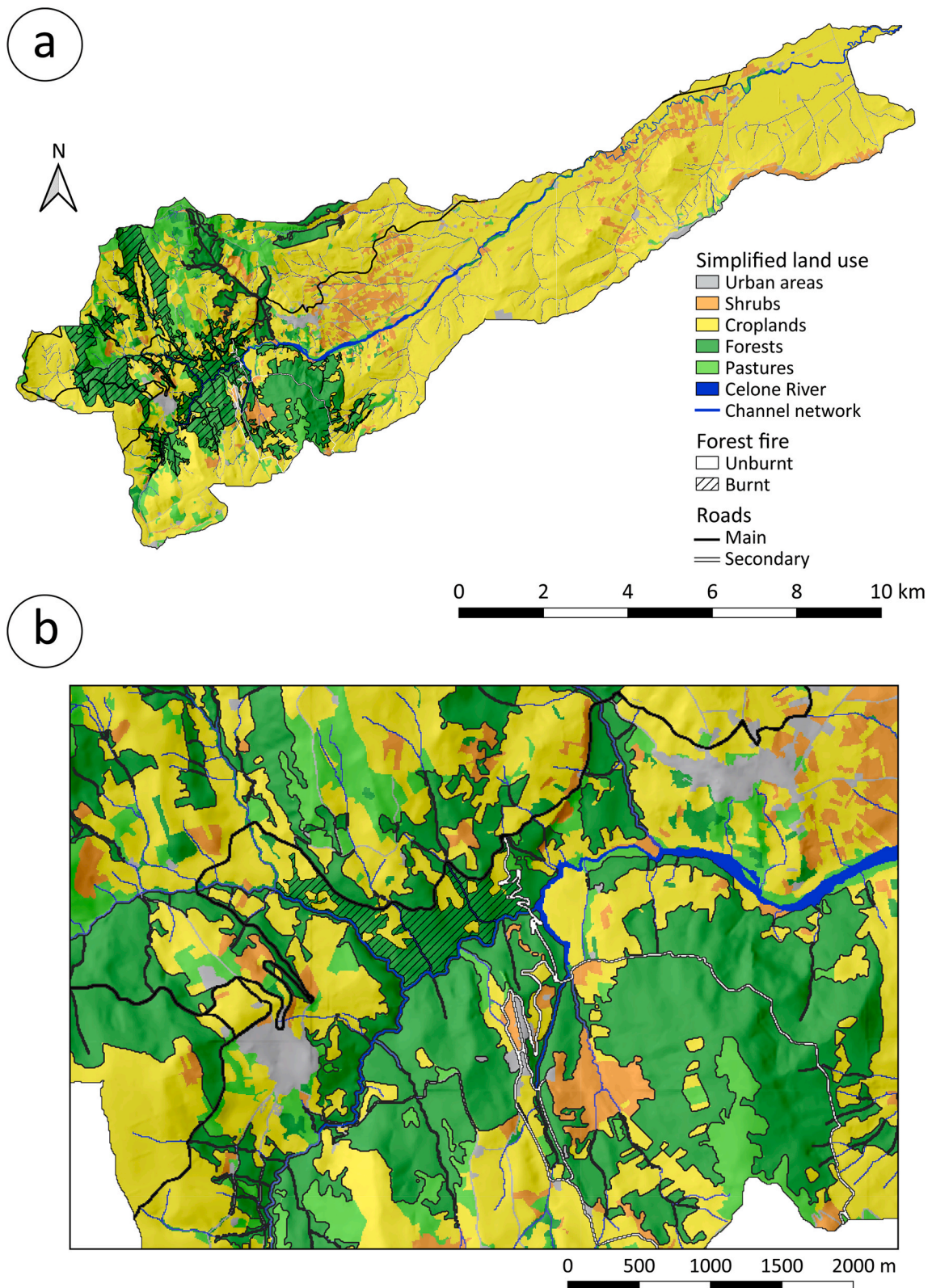


Fig. 2. Land use and illustration of one forest fire configuration for a) scenario 2 and b) scenario 8 (zoomed on the upper part of the catchment). In b), note that the unique forest patch was divided by both the Celone River in the southern part and by the main road (black) in the upper part. The reader is referred to the Supplementary material for the detailed figures of each scenario.

Table 1

Description of the land-use scenarios used in this study. Scenario 1 is corresponding to model calibration. All fire scenarios (scenarios 2 to 8) include the 15-m radius condition. The mean burnt area is presented as absolute area (km²) and relative to the total catchment area (%).

Scenarios	Fire breaks – Number of burnt forest patches	Forest patches splitting conditions	Mean burnt area
1	No – 0	No forest fire (Baseline scenario)	0 km ² –0%
2	No – 7	Within 15 m radius	1.44 km ² –2%
3	Yes – 10	Secondary road	1.09 km ² –1.5%
4	Yes – 15	Secondary road + river	1.09 km ² –1.5%
5	Yes – 11	Main road	0.80 km ² –1.1%
6	Yes – 15	Main road + river	0.80 km ² –1.1%
7	Yes – 15	Main road + secondary road	0.80 km ² –1.1%
8	Yes - 19	Main road + secondary road + river	0.63 km ² –0.9%

capacity decreasing from 60 mm h⁻¹ to 30 mm h⁻¹ (Cerdà, 1998; Robichaud, 2000), Manning's *n* decreasing from 0.4 to 0.3 (Nunes et al., 2018), and soil erodibility (in the WaterSed model representing both the soil cover and the intrinsic soil erodibility) increasing by a factor of 12 (De Girolamo et al. in prep.).

2.6. Model performance evaluation

The model was calibrated by comparing the measured and simulated water volumes and sediment loads over the 21 flood events. One exceptional event occurred in March 2011: the measured water volume was approximately nine times the mean of the 20 other events and approximately 30 times the sediment load of the other events. To prevent achieving good calibration only because of a correct simulation of this exceptional event, a leave-one-out procedure was adopted. The model was calibrated two times: with and without this extreme event. The corresponding calibrated values were those that resulted in better calibration in both cases. Calibration was evaluated using the coefficient of determination (R²), Nash-Sutcliffe index and percentage bias (Moriassi et al., 2007; Nunes et al., 2018).

3. Results and discussion

3.1. Model calibration

The model performance in the baseline run is described in Table 2.

The model calibration was good even for the extreme event, as reflected by the two calibration procedures. The model performance was lower when removing extreme events, as reflected by the leave-one-out results, exhibiting Nash-Sutcliffe indices of 0.90 and 0.86 and Pbias values smaller than 4% for the water volume (Fig. 3a) and sediment load (Fig. 3b), respectively.

Considering the water volume, the high Pbias value (–11%) indicated that the model overestimated the water volume, particularly for the high magnitude event, indicating that the water yield could be

Table 2

Model performance using the 21 recorded flood events (“all events”) and without the extreme event (“leave-one-out”).

Variable - Events used	R ² (–)	Nash-Sutcliffe index (–)	Pbias (%)
Water volume – all events	0.96	0.75	–11.00
Water volume – leave-one-out	0.77	0.90	0.30
Sediment load – all events	0.99	0.99	3.27
Sediment load – leave-one-out	0.74	0.86	3.70

improved. Nevertheless, as this study focuses on sediment loads and considering the lower Pbias obtained when removing this event from the calibration procedure, the overall model calibration was considered acceptable.

3.2. Forest fire consequences on sediment yield

The forest patches were defined and burnt based on the scenarios defined in Table 1, resulting in various burnt locations and areas (Fig. 2 and Supplementary material). The resulting burnt areas were, depending on the considered scenarios, between 3 and 613 ha, corresponding to the model runs with the smallest burnt patch (included in scenario 8) to the largest burnt patch (included in scenario 2), respectively. They were, on mean over the different model runs, ranging from 144 ha for scenario 2 (largest patch areas) to 63 ha for scenario 8 (smaller patch areas).

Although forest fires affected small catchment areas, corresponding to an average of 1%–2% of the catchment area and up to a maximum of 9%, they increased the mean sediment yield by 5% and up to a maximum of 37%. Indeed, the modelled sediment yields ranged from 1.97 t ha⁻¹.yr⁻¹ to 2.7 t ha⁻¹.yr⁻¹, depending on the burnt area (Fig. 4).

This increase in sediment yield because of forest fire remained low compared to the modelling results of Nunes et al. (2018), who reported that the modelled sediment yield increased from 0.14 t ha⁻¹.yr⁻¹ to 2.1 t ha⁻¹.yr⁻¹ after forest fires occurred on pines and eucalyptus in a catchment where 10% of the total area was burned. Although it has been reported that forest fires could induce contrasting effects and result in large sediment export ranges (Smith et al., 2011), these differences can be explained by the differences between the two catchments' land uses and the differences in modelling tools. In our study, forests represented a smaller proportion of the catchment area and a higher proportion of crops; agricultural lands and forests represented 55% and 37% of the total catchment area, respectively. In the study by Nunes et al. (2018), agricultural lands and forests represented 30% and 60%, respectively. While agricultural land exhibited lower erosion rates than those of burnt areas, they provided most of the sediment flux “baseline” (i.e., the intercept in Fig. 4a). Moreover, in our study, agricultural fields and most of the forests were directly connected to the Celone River. It was therefore not surprising that the baseline was higher, and consequently, the relative increase due to forest fires was lower.

Basso et al. (2019) indicated that in a catchment of similar shape and land cover, forest fires increased the sediment yield from 1.53 t ha⁻¹.yr⁻¹ to 1.74 t ha⁻¹.yr⁻¹ (14% increase with 69% of burnt catchment area) at the sub-basin scale (20,815 ha). Interestingly, in our study, the values were on the same order of magnitude for both the sediment yield and the increase due to forest fires. Although the burnt area proportion was higher in their study, the larger catchment area was likely to have resulted in a higher deposition rate and therefore smaller sediment yield (Delmas et al., 2012). They also reported the sediment yield increased from 0.75 t ha⁻¹.yr⁻¹ to 1.44 t ha⁻¹.yr⁻¹ at the catchment scale, however at a much larger scale (almost 300,000 ha), preventing a comparison with the values from our study.

Moreover, using a unique four-year monitoring period at the catchment scale including pre- and post-fire measurements, Nunes et al. (2020) reported post-fire sediment yields ranging from 0.01 t ha⁻¹.yr⁻¹ to 0.43 t ha⁻¹.yr⁻¹. Our results, corresponding to a 0.63 t ha⁻¹.yr⁻¹ increase, are on the same order of magnitude, although higher, which may be explained by the channel network extent, which extends over the entire catchment in our study. This extension increased the sediment connectivity and transfer to the catchment outlet. This high connectivity was reflected by the almost linear relationship observed between the burnt area and the sediment yield. The R² was 0.99 for the total regression and 0.98 if the five highest points were removed, and both regressions were significant at the 1% level of significance. The residuals (Fig. 4b) indeed indicated that the dispersion remained low. The mean squared error was 1.3%, and the residuals were normally distributed (p-value was 6.10⁻⁹) and ranged from –2.5 x 10⁻² t ha⁻¹.yr⁻¹ to 6.8 x

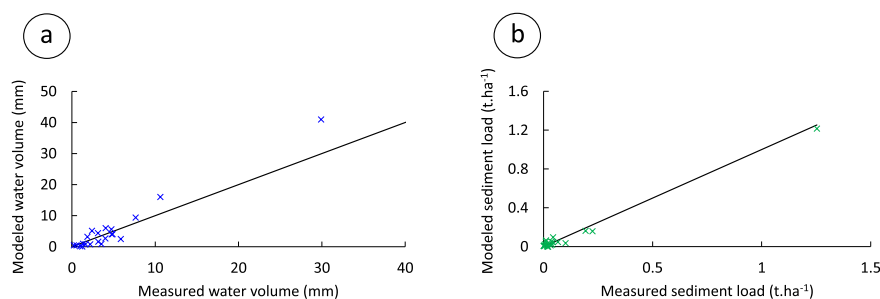


Fig. 3. Results of the 21 modelled flood events for a) water volume and b) sediment load.

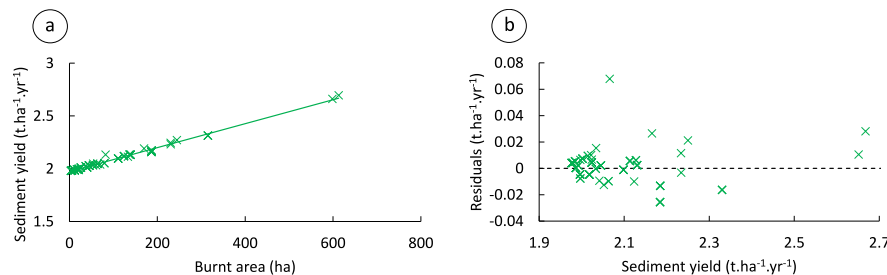


Fig. 4. a) Relationship between the annual sediment yield and burnt area, including the 21 flood events, for all model runs including forest fires and b) the associated regression residuals. The dotted line in b) indicates the null residuals.

$10^{-2} \text{ t ha}^{-1} \cdot \text{yr}^{-1}$. The spatial distribution of burnt patches therefore had minor impacts on the catchment sediment yield (on the order of $10^{-2} \text{ t ha}^{-1} \cdot \text{yr}^{-1}$).

This result was linked to the direct connection between the forest patches and the streams, resulting in limited deposition on hillslopes, and was in line with the connectivity index variations over the different scenarios (Fig. 5).

The connectivity index ranged from -6.18 to -5.83 in all scenarios and decreased with decreasing burnt area. The maximum value decreased from -5.83 in scenario 2 (larger burnt area) to -5.96 in scenario 8 (smaller burnt area), representing relatively small variations in the connectivity index. Interestingly, the connectivity index increased because of forest fires, indicating that although the burnt areas were small, they did significantly affect sediment connectivity.

Baartman et al. (2020) demonstrated that the spatial pattern of

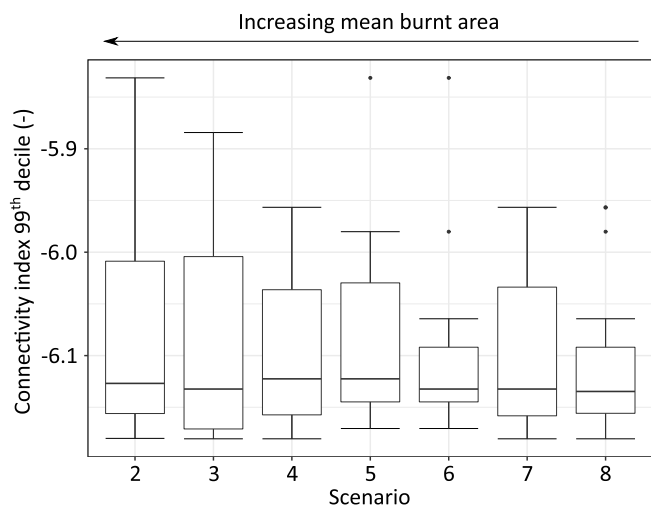


Fig. 5. Boxplot of connectivity index 99th decile for the modelled scenarios. The mean burnt areas increased from scenario 8 to scenario 2.

eroding fields had little consequence on the modelled catchment sediment yield at the outlet of a semi-virtual 124 ha agricultural loess catchment under various field allocations and for important rainfall depths (i.e., rainfall return period was 10 years and 50 years in their study). The authors, however, noted that this result was model-dependent, underlining the need to perform additional studies addressing the effects of the spatial pattern of erosion and sediment transport at the catchment scale. In the current study, we extended the results Baartman et al. (2020) obtained using the WaterSed model using 21 measured flood event datasets and a contrasted catchment. Indeed, our study was performed on a larger catchment area and included highly variable slopes and multiple spatial sediment sources of highly contrasting erosion behaviour, including a mountainous and forested part with various forest fire scenarios and a cultivated plain.

From a practical point of view, this result suggested that, in our study, the most efficient way to reduce forest fire effects on sediment yield was to decrease the size of the burnt area, using firebreaks to prevent fire extension (Fig. 6).

Indeed, the maximum sediment yield, corresponding to a worst-case model run, decreased from $2.70 \text{ t ha}^{-1} \cdot \text{yr}^{-1}$ in scenario 2 to $2.17 \text{ t ha}^{-1} \cdot \text{yr}^{-1}$ in scenario 8, and the maximum burnt area decreased from 613 to 187 ha because of firebreaks. The burnt area and the use of firebreaks were therefore demonstrated to significantly affect the sediment yield at the catchment and annual scales, contributing to a 20% decrease at the annual scale in the worst-case model run.

3.3. Analysis at the flood event scale

Previous studies noted that, particularly in headwater mountainous catchments, most of the sediment yield occurs during the most severe storm events (e.g., Navratil et al., 2011). This behaviour was also measured in the Celone catchment (De Girolamo et al., 2015). Indeed, the sediment load was found to correlate well ($R^2 = 0.8$) with the peak discharge, in agreement with previous studies performed in headwater catchments (Duvert et al., 2012). In our study, the peak discharge ranged from $1.7 \text{ m}^3 \text{ s}^{-1}$ to $30.2 \text{ m}^3 \text{ s}^{-1}$, underlining the variety of recorded flood events. To analyse the process affecting sediment

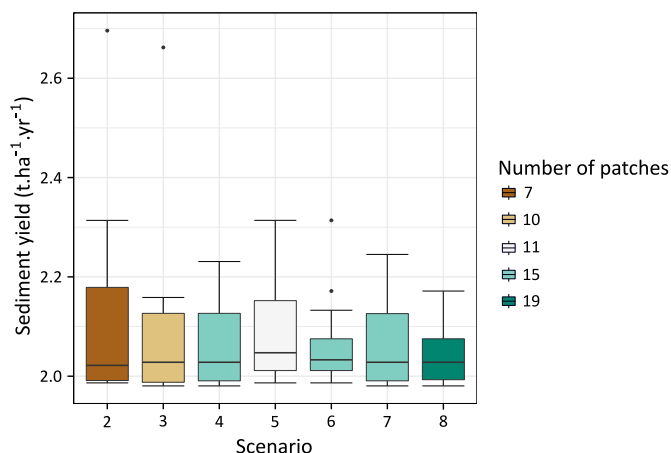


Fig. 6. Boxplot of the sediment yield in the various model runs by scenario. The number of forest patches is indicated by the boxplot colours. (For interpretation of the references to colour in this figure legend, the reader is referred to the Web version of this article.)

transport at the catchment scale, we focused on analysing the different flood events that occurred during the monitoring period.

For scenario 2, the mean sediment load increased by more than 130% relative to the baseline load for 11 of the modelled flood events. It increased up to 154% for an event of important magnitude, resulting from a 64 mm rainfall event, while the median rainfall depth recorded over the 21 flood events was 20.7 mm. The corresponding flood event resulted in more than three days of flood events with associated high runoff: the measured runoff was 54% higher than the median over the 21 events, and the maximum recorded peak discharge was 30.2 m³ s⁻¹, while the mean was 8.3 m³ s⁻¹. This effect was clearer when considering the maximum sediment load modelled over the various flood events. Indeed, 48% of the modelled flood events displayed maximum sediment loads ranging from 110% to 324% of the baseline scenario sediment load. This result underlines that the rainfall-flood event characteristics significantly affect sediment production and delivery to the river channel and then to the catchment outlet. The effects of increasing firebreak length in contact with forests on sediment load at the flood event scale are illustrated in Fig. 7.

The median of the sediment loads of the 21 flood events decreased from 136% of the baseline sediment load in scenario 2 (no firebreaks) to 111% in scenario 8 (when both the river channel and the two roads were considered to act as firebreaks). The effects of firebreaks were particularly important for the most important flood events. Indeed, the worst-case flood event, in which the maximum sediment load was 324% of the baseline scenario, was significantly decreased to 165%. Of note,

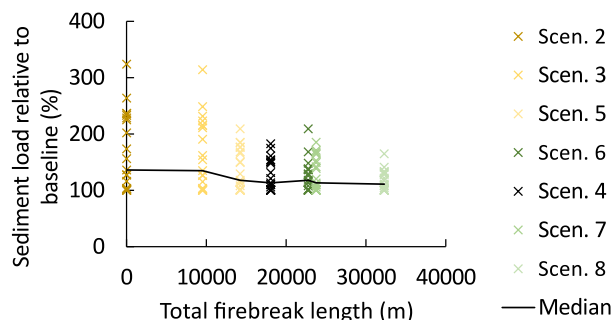


Fig. 7. Relationship between event-scale sediment load, relative to the baseline, and the length of the firebreaks in each scenario. The black continuous line indicates the median of the scenarios. Please note that the reported values indicate the length in contact with forest that was considered for forest fire.

scenario 4, which included the secondary road and the main river channel as firebreaks, provided interesting results, decreasing the median to 113% and particularly decreasing the worst-case flood event to 183%. The results in this scenario were similar to those of scenario 7, which included the main and secondary roads. The similarity can be explained by the proximity of the road with the river channel and implies that maintaining only small parts of the catchments as firebreaks can significantly reduce the effects of forest fires. This result underlined the important firebreak effects on the sediment load of major flood events occurring in catchments in relation to the spatial distribution of forest fire patches, at least in this study's configuration.

Cawson et al. (2013) previously demonstrated the effects of burnt-unburnt patchiness on runoff and erosion at the hillslope scale. Our study suggested that increasing the burnt-unburnt patchiness might lead to significantly decreased sediment loads at the catchment scale. Therefore, regardless of the forest fire configuration and flood event characteristics (as simulated in this study), maintaining firebreaks based on existing manmade and natural features resulted in limiting forest fire effects and should therefore help limit the deleterious effects of fire on water quality (White et al., 2006).

It should be noted that, on average, the rainfall and flood event characteristics (reported in the Supplementary material) had higher consequences on sediment load variations than the effects of firebreak locations and forest fire extent. Indeed, focusing on the two extreme scenarios (i.e., scenario 2 and scenario 8), the mean sediment load varied over the different burnt patches from 100% to 154%, with an average of 115% of the baseline sediment load in scenario 2, and from 100% to 122%, with an average of 106% in scenario 8. Higher variations were therefore modelled between flood events than between scenarios, as reflected by the boxplot extent in Fig. 6 and the dispersion in Fig. 7. This result corroborated the findings of Baartman et al. (2020), who demonstrated that rainfall characteristics played the most important role in determining the relative sediment export in a very different context and for contrasting rainfall characteristics. This result was also in line with the experimental study by Nunes et al. (2020), who found that storm characteristics dominated streamflow and sediment yield changes in a burnt catchment. This result indicated that rainfall, in this study ranging from 3 mm to 64 mm (mean 22 mm), and the resulting flood event characteristics, might be of prior importance to analyse in studies analysing sediment export and sediment connectivity.

3.4. Main results and management implications

In this study, the effects of forest fires on sediment load were studied at the catchment scale. The results obtained might be site-dependent, but they were obtained using a realistic approach, using multiple plausible fire scenarios and firebreak locations. Therefore, the results should be robust. Moreover, the use of measured rainfall, discharge and suspended sediment concentration data allowed the study of fire and firebreak effects over multiple flood event characteristics.

The spatial configuration of the burnt-unburnt patches, and more generally of sediment sources in the catchment, was illustrated in this study. This result implied that it is important to consider this variability to understand sediment load variations. In this study, the burnt area mainly controlled the sediment load variations, but it was of second order relative to the rainfall-flood event characteristics. Interestingly, firebreaks were demonstrated to be able to greatly reduce sediment load, particularly in the case of the most severe storm event. The burnt patch locations were suggested to be of third order, resulting in limited sediment load variations.

This result indicated that it is of critical importance to avoid fire propagation over large areas but that the location of the burnt areas does not significantly affect sediment load. Moreover, the almost linear relationship found between burnt areas and the increase in sediment load suggested that fires might generate transport-limited conditions in the catchment.

Consequently, preventing erosion and downstream negative effects should be done i) by limiting fire extent ii) with little importance (relative to erosion and sediment transport) of the burnt locations and iii) particularly prior to severe storm events, while limited export increase should be expected following minor rainfall events.

More generally, models such as the one used in this study may be helpful tools that can be used to plan mitigation strategies. The model can be used to design firebreak locations or to test the effects of implanting soft hydraulic conservation measures, such as linear vegetative filters, after fires to limit fire effects on sediment loads.

4. Conclusions

Forests provide many natural services that are threatened by the increasing probability of forest fires, particularly in the Mediterranean region. Numerical models should therefore be developed to help design adequate mitigation strategies against deleterious forest fire effects, such as soil erosion and sediment transfer to downstream environments.

This study proposed the adaptation of a runoff and erosion model to the case of forest fires. The model was then used to analyse the effects of fires on sediment yield under various fire scenarios, including a variety of firebreaks, and for 21 flood events representing an entire hydrological year. The catchment sediment load was found to increase with the mean burnt areas, from $1.97 \text{ t ha}^{-1}\cdot\text{yr}^{-1}$ to $2.70 \text{ t ha}^{-1}\cdot\text{yr}^{-1}$, even when these were low. This result suggested the importance of forest fires on the catchment sediment budget.

Realistic firebreak strategies, considering the main roads acting as firebreaks, were shown to significantly reduce the sediment load increase induced by fires. It was found that increasing burnt area patchiness and reducing burnt areas resulted in smaller sediment loads. The importance of the rainfall and flood characteristics, relative to the land use and particularly burnt-unburnt forests, was underlined, although firebreaks were found to significantly decrease the effects of the worst-case model runs. The burnt patch location was found to have a limited impact on the sediment load.

This study represented a realistic situation, with croplands on the catchment plain and forests on steep lands that can hardly be turned into other land uses. Moreover, this catchment is mostly rural and likely to experience land abandonment in the future. This process will likely result in increased land conversion to forests. Such an increase in forested areas is expected to be beneficial for the environment, especially considering erosion and sediment loads. However, forest fires could punctually balance these positive effects. There is therefore a need to use adequate numerical tools to design remediation strategies that can balance the negative effects of fire and achieve an overall positive effect.

Credit Authors Statement

[All co-authors conceptualized the study]. TG, RV and OC designed the simulations and wrote the initial draft. TG performed the simulations and finalised the writing. [AMDG, RV and TG collected and prepared the SIG data... etc. All co-authors reviewed the paper. TG wrote the revised manuscript. RV, OC, AMDG and ALP secure funding and were involved in project administration.

Declaration of competing interest

The authors declare that they have no known competing financial interests or personal relationships that could have appeared to influence the work reported in this paper.

Acknowledgements

This study was funded by the ERA4CS SERV_FORFIRE project. ERA4CS is an ERA-NET initiated by JPI Climate, and funded by FORMAS (SE), DLR (DE), BMFW (AT), IFD (DK), MINECO (ES), ANR (FR) with

co-funding by the European Union (Grant 690462). Florian Masson and Valentin Landemaine are gratefully acknowledged for providing advice on the figures provided in the Supplementary material. The reviewers provided interesting comments that helped improve the manuscript quality.

Appendix A. Supplementary data

Supplementary data to this article can be found online at <https://doi.org/10.1016/j.jenvman.2021.112497>.

References

- Baartman, J.E.M., Nunes, J.P., Masselink, R., Darboux, F., Bielders, C., Degre, A., Cantreul, V., Cerdan, O., Grangeon, T., Fiener, P., Wilken, F., Schindewolf, M., Wainwright, J., 2020. What do models tell us about water and sediment connectivity? *Geomorphology* 367, 1073000. <https://doi.org/10.1016/j.geomorph.2020.107300>.
- Basso, M., Vieira, D.C.S., Ramos, T.B., Mateus, M., 2019. Assessing the adequacy of SWAT model to simulate postfire on the watershed hydrological regime and water quality. *Land Degrad. Dev.* 31, 619–631.
- Borrelli, P., Panagos, P., Langhammer, J., Apostol, B., Schütt, B., 2016. Assessment of the cover changes and the soil loss potential in European forestland: first approach to derive indicators to capture the ecological impacts on soil-related forest ecosystems. *Ecol. Indic.* 60, 1208–1220.
- Borselli, L., Cassi, P., Torri, D., 2008. Prolegomena to sediment and flow connectivity in the landscape: a GIS and field numerical assessment. *Catena* 75, 268–277.
- Bredemeir, M., 2011. Forest, climate and water issues in Europe. *Ecohydrology* 4, 159–167.
- Cavalli, M., Trevisani, S., Comiti, F., Marchi, L., 2013. Geomorphic assessment of spatial sediment connectivity in small Alpine catchments. *Geomorphology* 188, 31–41.
- Cawson, J.G., Sheridan, G.J., Smith, H.G., Lane, P.N.J., 2013. Effects of fire severity and burn patchiness on hillslope-scale surface runoff, erosion and hydrologic connectivity in a prescribed burn. *For. Ecol. Manag.* 310, 219–233.
- Cerdà, A., 1998. Changes in overland flow and infiltration after a rangeland fire in a Mediterranean scrubland. *Hydrol. Process.* 12, 1031–1042.
- Certini, G., 2005. Effects of fire on properties of forest soils: a review. *Oecologia* 143, 1–10.
- Chapman, T.G., 1991. Comment on "Evaluation of automated techniques for base flow and recession analyses". In: Nathan, R.J., McMahon, T.A. (Eds.), *Water Resources Research* 27, 1783–1784. <https://doi.org/10.1029/91WR01007>.
- Civil Protection Agency, 2018. Regional Plan 2018–2020. <https://protezionecivile.puglia.it/publicazioni-incendi/piano-regionale-aib-2018-2020>. (Accessed 23 November 2020).
- Crema, S., Cavalli, M., 2018. SedInConnect: a stand-alone, free and open source tool for the assessment of sediment connectivity. *Comput. Geosci.* 111, 39–45.
- Cui, X., Amal, M.D.A., Perry, G.L.W., Paterson, A.M., Wyse, S.V., Curran, T.J., 2019. Green firebreaks as a management tool for wildfires: lessons from China. *J. Environ. Manag.* 233, 329–336.
- Curran, T.J., Perry, G.W.L., Wyse, S.V., Alam, M.A., 2018. Managing fire and biodiversity in the wildland-urban interface: a role for green firebreaks. *Fire*. <https://doi.org/10.3390/fire1010003>.
- De Girolamo, A.M., Pappagallo, G., Lo Porto, A., 2015. Temporal variability of suspended sediment transport and rating curves in a Mediterranean river basin: the Celone (SE Italy). *Catena* 126, 135–143.
- De Girolamo, A.M., Bouroui, F., Buffagni, A., Pappagallo, G., Lo Porto, A., 2017. Hydrology under climate change in a temporary river system: potential impact on water balance and flow regime. *River Res. Appl.* 33, 1219–1232. <https://doi.org/10.1002/rra.3165>.
- De Girolamo, A.M., Di Pillo, R., Lo Porto, A., Todisco, M.T., Barca, E., 2018. Identifying a reliable method for estimating suspended sediment load in a temporary river system. *Catena* 165, 442–453. <https://doi.org/10.1016/j.catena.2018.02.015>.
- De Walque, B., Degré, A., Maignard, A., Bielders, C.L., 2017. Artificial surfaces characteristics and sediment connectivity muddy flood hazard in Wallonia. *Catena* 158, 89–101.
- Delmas, M., Pak, L.T., Cerdan, O., Souchère, V., Le Bissonnais, Y., Couturier, A., Sorel, L., 2012. Erosion and sediment budget across scale: a case study in a catchment of the European loess belt. *J. Hydrol.* 420–421, 255–263.
- Duvert, C., Nord, G., Gratiot, N., Navratil, O., Nadal-Romero, E., Mathys, N., Némery, J., Regüés, D., García-Ruiz, J.M., Gallart, F., Esteves, M., 2012. Towards prediction of suspended sediment yield from peak discharge in small erodible mountainous catchments (0.45–22 km²) of France, Mexico and Spain. *J. Hydrol.* 454–455, 42–55.
- Esteves, T.C.J., Kirby, M.J., Shakesby, R.A., Ferreira, A.J.D., Soares, J.A.A., Irvine, B.J., Ferreira, C.S.S., Coelho, C.O.A., Bento, C.P.M., Carreiras, M.A., 2012. Mitigating land degradation caused by wildfire: application of PESERA model to fire-affected sites in central Portugal. *Geoderma* 191, 40–50.
- European Environment Agency, 2019. Burnt Area in European Countries. https://www.eea.europa.eu/data-and-maps/daviz/burnt-forest-area-in-five-2#tab-chart_4. (Accessed 10 February 2021).
- Farley, K., Jobbagy, E.G., Jackson, R.B., 2005. Effects of afforestation on water yield: a global synthesis with implications for policy. *Global Change Biol.* 11, 1565–1576.

- Fernández, C., Vega, J.A., 2016. Evaluation of RUSLE and PESERA models for predicting soil erosion losses in the first year after wildfire in NW Spain. *Geoderma* 273, 64–72.
- Fernández, C., Vega, J.A., Vieira, D.C.S., 2010. Assessing soil erosion after fire and rehabilitation treatments in NW Spain: performance of RUSLE and revised Morgan-Morgan-Finney models. *Land Degrad. Dev.* 21, 774–787.
- Fernández, C., Fernández-Alonso, J.M., Vega, J.A., 2020. Exploring the effect of hydrological connectivity and soil burn severity on sediment yield after wildfire and mulching. *Land Degrad. Dev.* 31 (13), 1611–1621.
- Flannigan, M., Krawchuk, M., de Groot, W., Wotton, B., Gowman, L., 2009. Implications of changing climate for global wildland fire. *Int. J. Wildland Fire* 18, 483–507.
- Gabriels, D., Ghekiere, G., Schiettecatte, W., Rottiers, I., 2003. Assessment of USLE cover-management C-factors for 40 crop rotations systems on arable farms in the Kemmelbeek watershed, Belgium. *Soil Tillage Res.* 74 (1), 47–53.
- Grangeon, T., Manière, L., Foucher, A., Vandromme, R., Cerdan, O., Evrard, O., Pene-Galland, I., Salvador-Blanes, S., 2017. Hydro-sedimentary dynamics of a drained agricultural headwater catchment: a nested monitoring approach. *Vadose Zone J.* 16 (12) <https://doi.org/10.2136/vzj2017.05.0113>.
- ISPRA, 2020. Italian Environmental Data Yearbook 2019. Sistan 93 Bis (2020). <https://annuario.isprambiente.it/sites/default/files/pdf/2019/Italian-Environment.pdf>. (Accessed 10 December 2020).
- ISTAT, 2010. Pressione degli incendi sull'ambiente – anni 1970-2009. Ambiente e Territorio, 22/06/2010. <https://www.istat.it/it/files//2011/01/testointegrale20100622.pdf>. (Accessed 10 December 2020).
- Kamps, S.K., Gannon, B.M., Wilson, C., Saavedra, F., Miller, M.E., Heldmyer, A., Livneh, B., Nelson, P., MacDonald, L., 2020. PEMIP: post-fire erosion model inter-comparison project. *J. Environ. Manag.* 268, 110704.
- Landemaine, V., Cerdan, O., Grangeon, T., Vandromme, R., Laignel, B., Evrard, O., Salvador-Blanes, S., Lacey, P., Saturation-excess overland flow in the European loess belt: an underestimated process? In Prep.
- Larsen, L.J., MacDonald, L.H., 2007. Predicting post-fire sediment yields at the hillslope scale: testing RUSLE and Disturbed WEPP. *Water Resour. Res.* 43, W11412.
- Martin, D.A., Moddy, J.A., 2001. Comparison of soil infiltration rates in burned and unburned mountainous watershed. *Hydrol. Process.* 15, 2893–2903.
- Matsypura, D., Prokopyev, O.A., Zahar, A., 2018. Wildfire fuel management: network-based models and optimization of prescribed burning. *Eur. J. Oper. Res.* 264, 774–796.
- Mayor, A.G., Bautista, S., Llovet, J., Bellot, J., 2007. Post-fire hydrological and erosional responses of a Mediterranean landscape: seven years of catchment-scale dynamics. *Catena* 71, 68–75.
- Moriassi, D.N., Arnold, J.G., Van Liew, M.W., Bingner, R.L., Harmel, R.D., Veith, T.L., 2007. Model evaluation guidelines for systematic quantification of accuracy in watershed simulations. *Transactions of the ASABE* 50, 885–900.
- Morvan, D., 2015. Numerical study of the behavior of a surface fire propagating through a firebreak built in a Mediterranean shrub layer. *Fire Saf. J.* 71, 34–48.
- Navratil, O., Esteves, M., Legout, C., Gratiot, N., Némery, J., Willmore, S., Grangeon, T., 2011. Global uncertainty analysis of suspended sediment monitoring using turbidimeter in a small mountainous river catchment. *J. Hydrol.* 398, 246–259.
- Nunes, J.P., Quintanilla, P.N., Santos, J.M., Serpa, D., Carvalho-Santos, C., Rocha, J., Keizer, J.J., Keestra, S.D., 2018. Afforestation, subsequent forest fires and provision of hydrological services: a model-based analysis for a Mediterranean mountainous catchment. *Land Degrad. Dev.* 29, 776–788.
- Nunes, J.P., Bernard-Jannin, L., Rodríguez-Blanco, M.L., Boulet, A.K., Marisa Santos, J., Keizer, J.J., 2020. Impacts of wildfire and post-fire land management on hydrological and sediment processes in a humid Mediterranean headwater catchment. *Hydrol. Process.* <https://doi.org/10.1002/hyp.13926>.
- Ortiz-Rodríguez, A.J., Muñoz-Robles, C., Borselli, L., 2019. Changes in connectivity and hydrological efficiency following wildland fires in Sierra Madre Oriental, Mexico. *Sci. Total Environ.* 655, 115–128.
- Oudin, L., Hervieu, F., Michel, C., Perrin, C., Andréassian, V., Anctil, F., Loumagne, C., 2005. Which potential evapotranspiration input for a lumped rainfall-runoff mode? Part 2 – towards a simple and efficient potential evapotranspiration model for rainfall-runoff modelling. *J. Hydrol.* 303, 290–306.
- Owens, P.N., Batalla, R.J., Collins, A.J., Gomez, B., Hicks, D.M., Horowitz, A.J., Kondolf, G.M., Marden, M., Page, M.J., Peacock, D.H., Petticrew, E.L., Salomons, W., Trustrum, N.A., 2005. Fine-grained sediment in river systems: environmental significance and management issues. *River Res. Appl.* 21, 693–717.
- Pausas, J.G., 2004. Changes in fire and climate in the eastern Iberian Peninsula (Mediterranean basin). *Climatic Change* 63, 337–350.
- Pausas, J.G., Keeley, J.E., 2009. A burning story: the role of fire in the history of Life. *Biosciences*, 59, 593–601.
- Pausas, J.G., Llovet, J., Rodrigo, A., Vallejo, R., 2008. Are wildfires a disaster in the Mediterranean basin? – a review. *Int. J. Wildland Fire* 17 (6), 713–723.
- Puglia, Regione, 2016. Legge N. 38: Norme in materia di contrasto agli incendi boschivi di interfaccia 12/12/2016. *Bollettino Regione Puglia n° 143* pubblicato il 14-12-2016.
- Robichaud, P.R., 2000. Fire effects on infiltration rates after prescribed fire in Northern Rocky Mountain Forests, USA. *J. Hydrol.* 231–232, 220–229.
- Robichaud, P.R., Elliot, W.J., Pierson, F.B., Hall, D.E., Moffet, C.A., 2007. Predicting postfire erosion and mitigation effectiveness with a web-based probabilistic erosion model. *Catena* 71, 229–241.
- Salis, M., Del Giudice, L., Robichaud, P.R., Ager, A.A., Canu, A., Duce, P., Pellizzaro, G., Ventura, A., Alcasena-Urdiroz, F., Spano, D., Arca, B., 2019. Coupling wildfire spread and erosion models to quantify post-fire erosion before and after fuel treatments. *Int. J. Wildland Fire.* <https://doi.org/10.1071/WF19034>.
- Saulnier, G.M., Beven, K., Obléd, C., 1997. Including spatially variable effective soil depths in TOPMODEL. *J. Hydrol.* 202, 158–172. [https://doi.org/10.1016/S0022-1694\(97\)00059-0](https://doi.org/10.1016/S0022-1694(97)00059-0).
- Schüler, G., 2006. Identification of flood-generating forest areas and forestry measures for water retention. *For. Snow Landsc. Res.* 80, 99–114.
- Scott, R.E., Neyland, M.G., McElwee, D.J., Baker, S.C., 2012. Burning outcomes following aggregated retention harvesting in old-growth wet eucalyptus forests. *For. Ecol. Manag.* 276, 165–173.
- Shakesby, R.A., 2011. Post-wildfires erosion in the Mediterranean: review and future research directions. *Earth Sci. Rev.* 105, 71–100.
- Smith, R., 2014. Firebreak Location, Construction and Maintenance Guidelines. Bush Fire and Environmental Protection Branch, p. 25.
- Smith, H.G., Sheridan, G.J., Lane, P.N.J., Nyman, P., Haydon, S., 2011. Wildfire effects on water quality on forest catchments: a review with implications for water supply. *J. Hydrol.* 396, 170–192.
- Thornthwaite, C.W., 1948. An approach toward a rational classification of climate. *Geogr. Rev.* 38 (1), 55–94. <https://doi.org/10.2307/210739>.
- Turco, M., Llasat, M.C., von Hardenberg, J., Provenzale, A., 2014. Climate change impacts on wildfires in a Mediterranean environment. *Climate Change.* <https://doi.org/10.1007/s10584-014-1183-3>.
- USDA, 1985. Soil Conservation Service, National Engineering Handbook. Section 4. Hydrology USDA-SCS, Washington DC.
- Van Eck, C.M., Nunes, J.P., Vieira, D.C.S., Keestra, S., Keizer, J.J., 2016. Physically-based modelling of the post-fire runoff response of a forest catchment in central Portugal: using field versus remote sensing based estimates of vegetation recovery. *Land Degrad. Dev.* 27, 1535–1544.
- Verkaik, I., Rieradevall, M., Cooper, S.D., Melack, J.M., Dudley, T.L., Prat, N., 2013. Fire as a disturbance in Mediterranean climate streams. *Hydrobiologia* 719, 353–382.
- Vieira, D.C.S., Prats, S.A., Nunes, J.P., Shakesby, R.A., Coelho, C.O.A., Keizer, J.J., 2014. Modelling runoff and erosion, and their mitigation, in burned Portuguese forest using the revised Morgan-Morgan-Finney model. *For. Ecol. Manag.* 314, 150–165.
- Vieira, D.C.S., Fernández, C., Vega, J.A., Keizer, J.J., 2015. Does soil burn severity affect the post-fire runoff and interrill erosion response? A review based on meta-analysis of field rainfall simulation data. *J. Hydrol.* 523, 452–464.
- Vieira, D.C.S., Serpa, D., Nunes, J.P.C., Prats, S.A., Neves, R., Keizer, J.J., 2018. Predicting the effectiveness of different mulching techniques in reducing post-fire runoff and erosion at plot scale with the RUSLE, MMF and PESERA models. *Environ. Res.* 165, 365–378.
- White, I., Wade, A., Worthy, M., Mueller, N., Daniell, T., Wasson, R., 2006. The vulnerability of water supply catchments to bushfires: impacts of the January 2003 wildfires on the Australian Capital Territory. *Aust. J. Water Resour.* 10 (2), 179–194.
- Wilson, A.A.G., 1988. Width of firebreak that is necessary to stop grass fires: some field experiments. *Can. J. For. Res.* 18 (6), 682–687.
- Wischmeier, W.H., Smith, D.D., 1978. Predicting rainfall erosion losses. Agriculture Handbook. Agricultural Research Service, US Department of Agriculture, Washington 537, 55.